



## Thermal characterization and diffusivity of two mono-component epoxies for transformer insulation

Juana Abenojar<sup>\*</sup>, Belén Enciso, Mariola Pantoja, Francisco Velasco, Miguel-Angel Martínez

Materials Science and Engineering and Chemical Engineering Dept, Universidad Carlos III de Madrid, Av. Universidad, 30, 28911, Leganés, Spain

### ARTICLE INFO

#### Keywords:

Mono-component resin  
Curing kinetic  
Degradation kinetic  
Thermal conductivity  
Durability

### ABSTRACT

The main aim of this study is the thermal characterization of an organic insulation. This insulation is a compound of two mono-component epoxy resins: *EpoxyLite*<sup>®</sup> primer and *ElmoTherm*<sup>®</sup> varnish. A mono-component epoxy resin usually needs a high temperature to cure; through differential scanning calorimetry (DSC) and thermogravimetric analysis (TGA), non-isothermal curves are obtained, allowing the estimation of activation energies of curing and decomposition processes respectively. If Model Free Kinetic (MFK) is used from DSC curves, it is possible to simulate isothermal curves at different temperatures and times, plotting activation energy as a function of the conversion degree. The simulation from TGA curves can be used to estimate lifetime of the resins and compare them following the Toop method. DSC also allows measurement of thermal conductivity, the melting peak of metallic gallium being used for this measurement. Finally, water diffusion in resins is studied. Currently, the Materials Performance research group of UC3M is working on the European project named "Essial", where this organic insulation is used to protect the windings and the whole transformer from the environment. The results obtained will be used to determinate the optimal operating range for this insulator, demonstrating that both epoxies are required to achieve the insulating performance of the transformer and long curing times are required for full curing of *EpoxyLite*<sup>®</sup>.

### 1. Introduction

The development of insulating liquids for heat dissipation has been very important for years, but this development stopped when oil-filled circuit cables were replaced by polypropylene cables [1]. However, the insulation of electrical machines and transformers has kept under development.

From the beginning of the seventies, epoxy resins have been used to insulate electrical apparatus from the environment. Previously, cellulosic-based insulators were used in the electrical industry for many years; materials like paper, cotton cloth or cotton tape were wound around the conductors. In order to have thinner insulators and to provide better electrical insulation, epoxy or phenolic-epoxy resins were introduced. Resinous materials (such as polyvinyl alcohol, phenolics, epoxies or phenolic-epoxies) were also employed together with cellulosic insulators [2]. The epoxy resin must hermetically seal the transformer and protect it against any external agents, like moisture, dust or dirt. It must protect the transformer from the most hostile environments, while offering the benefit of running cooler than a similar non-coated

transformer. EN 60529 [3] classifies and rates the degree of protection provided by enclosures against external agents, assigning an IP code (International Protection Marking). This code is formed by two digits. The first digit indicates protection against penetration by solid objects and the second is related to protection against penetration of water. The code may have an additional letter if the level of protection is better than that indicated by the first digit. Normally, for electrical transformers, IP65 is mandatory. This rating implies dust proof (first digit, 6) and protection against power water jets from any direction (second digit, 5). Therefore, epoxy protection systems are used to comply with this IP rating.

The excellent properties of epoxy resins (relating to chemical, mechanical and water resistance) have resulted in their widespread use in transformers. To achieve the properties required for this application, transformers are usually impregnated with epoxy resin, followed by in situ curing [4]. Another possible approach entails the impregnation of crepe paper with an epoxy resin [5]. Epoxy resins can have more applications in electrical insulation, such as multilayers in winding transformers [6], which are composed of several double-sided copper printed

<sup>\*</sup> Corresponding author.

E-mail address: [abenobar@ing.uc3m.es](mailto:abenobar@ing.uc3m.es) (J. Abenojar).

<https://doi.org/10.1016/j.ijadhadh.2020.102726>

Available online 9 September 2020

0143-7496/© 2020 The Author(s).

Published by Elsevier Ltd.

This is an open access article under the CC BY-NC-ND license

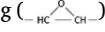
(<http://creativecommons.org/licenses/by-nc-nd/4.0/>).

circuit boards (bilayers) pressed and bonded together with an epoxy resin located between the bilayers.

Epoxy resins need to be applied under vacuum, since the presence of pores or cavities could cause voltage drops when increasing working temperature. This phenomenon could be explained by the dependency of the relative permittivity of the epoxy resin on the temperature as well as the diffusion processes on the cavity surroundings inside the epoxy resin [7]. Hikita et al. [8] found a decrease of discharge inception time in transformers with an increment of void diameter. The same effect was studied by Illias et al. [9], who developed a model for a single void, finding that the surface conductivity increases with the applied field and void size, as surface charge moves faster along the void wall, resulting in decreasing the electric field due to the surface charge.

It is also important to consider the classification of the insulating material based on the maximum continuous working temperature, established for 20 years of working life. The recommended temperature according to IEC 60034-1 [10] is lower than that to ensure an even longer life. When ambient temperature is about 60 °C during operation, F and H classes are normally used [11]. To isolate electrical transformers, the mandatory class is H and the protection is usually obtained by simple impregnation in a recommended insulating synthetic varnish without any organic fibres, followed by curing at a specified temperature and time.

Zhuang et al. [12] studied the lifetime for an epoxy resin insulated transformer at different voltages, predicting a 37-years lifetime for a full transformer at 90% confidence level and 90% reliability level. The electrical discharge endurance of an epoxy resin will be able to increase if it is cured by an acid anhydride in conjunction with a dispersion of silica nanoparticles [13].

Mono-component epoxy resins can avoid some drawbacks in comparison to bi-component resins, such as errors in the resin-hardener ratio or preparation at real time of the mixture [14]. Mono and bi-component resins have the same main components: epichlorohydrin and bisphenol A (or bisphenol F). Their reaction produces epoxy monomers (bisphenol A diglycidyl ether or bisphenol F diglycidyl ether, depending on the raw material). Then, reaction of epoxy monomers with primary or secondary (even if diamine) amines provides the opening of oxirane ring (). The amine is a nucleophile, its electrons attacking the electrophile part of oxirane rings (in this case carbon atom close to the oxirane ring oxygen, which is negatively charged, while the amine has a positive charge). This gives rise to the formation of a hydroxyl group (which catalyses the curing reaction [15]) and leaves an amine group on the molecule that allows the reaction to continue with another oxirane group. Another epoxide end group adds to the amine group, so on and so forth until a big molecular network is formed (the crosslinked network) [16]. Curing process to get the crosslinked network can be followed by differential scanning calorimetry (DSC), infrared spectroscopy (FTIR) or Raman spectroscopy among other techniques. Each technique needs a parameter to do calculus, as reaction heat, absorbance area, etc. The change of parameters with time provides the conversion degree ( $\alpha$ ). For example, by DSC,  $\alpha$  is defined according to Eq. (1), where  $\Delta H_t$  is the reaction heat for a certain time and  $\Delta H_T$  is the total reaction heat involved in an isothermal or non-isothermal process [17].

$$\alpha = \Delta H_t / \Delta H_T \quad (1)$$

To evaluate the conversion degree, different methods can be used, applying models to know kinetic parameters from empiric data, standing out Kamal and Kissinger methods. Kamal's method assumes two reaction mechanisms ( $n$  order and autocatalytic mechanisms) [18], while the Kissinger model proposes an  $n$  order mechanism with  $n = 1$  [19]. Kinetic models use an Arrhenius type equation to calculate the activation energy, starting from non-isothermal heatings (at different rates) or isothermal scans. The MFK model is based on the Vyazovkin model [20], providing information about the activation energy as a function of the conversion degree. The advantage of the MFK model is that it is possible

to simulate isothermal curves from non-isothermal tests and there is already software which allows calculus to know activation energy. MFK requires at least 3 different heating rates to determine the activation energy. As MFK deals with conversion degree and simulation is carried out at fixed temperatures, heating rates do not affect the results providing only one phenomenon (*i.e.*, curing) is being analysed. These methods can be used for both curing and decomposition reactions where there is a change over time [21].

Conversely, mono-component resins present some disadvantages such as the solvent amount; in some cases, this provokes their curing by evaporation of solvent, considering that the polymerization reaction was carried out previously. Besides, information on mono-component resins is so scarce that the use of such resin types is quite novel and thus it is necessary to study these high-temperature epoxy resins which can be used as protection for transformers. For this reason, the main objectives of this work are the understanding of their specific curing process, related, on the one hand, to the thermal properties (analysing their curing kinetics and activation energy), and on the other, to the chemical reactions; the influence of the curing process on the glass transition temperature ( $T_g$ ) of the resins; the evaluation of their thermal conductivity (a key factor for insulation); and the analysis of their decomposition kinetics and lifetime estimation. Besides, water diffusion in the resins is evaluated, studying them both separately and together (as they are going to be used).

## 2. Materials and methods

### 2.1. Materials

The epoxy resins used in this work were *Epoxilite*® 578 EB (named as EP) and the varnish *Elmotherm*® 6001 (named as TH), both supplied by Elantas UK Ltd (Manchester, United Kingdom). EP is an epoxy resin system, 180 °C class, designed for the impregnation of both random and form wound machines, and is suitable for use on windings rated up to and including 3.3 kV. It needs to be applied through a vacuum pressure impregnation process. According to the safety data sheet, EP includes: phenol, polymer with formaldehyde, oxiranylmethyl ether (between 30 and 50%), reaction product of bisphenol-A-(epichlorohydrin) and epoxy resin (average molecular weight  $\leq 700$ ) with a concentration between 30 and 50%, glyceryl polypropylene glycol ether (10–12.5%), 1,3-bis(2,3-epoxypropoxy)-2,2-dimethylpropane (5–7%) and trichloro (N,N-dimethyloctylamine)boron (3–5%).

TH is a mono-component epoxy with organic solvents (safety data sheet is not available), but other epoxy varnishes use a solvent mixture of ethanol, acetone, and methyl ethyl [22]. It is a class H varnish, which has excellent moisture and chemical resistance. It is applied by dipping or spraying, for rotating and non-rotating electrical and non-electrical equipment, over EP. When they are used as electrical transformer insulation, they are used together, and the system will be named EPTH within this research. Their viscosities at 25 °C are low, from 3000 to 5500 mPa s for EP and 300 mPa s for TH. Both need to be cured at high temperature. The curing cycle employed was 10 h at 140 °C for EP. Then TH was applied and the whole set was reheated for 10 h at 140 °C.

### 2.2. Kinetics (curing and decomposition processes) and glass transition temperature

To analyse the curing kinetic parameters of EP resin and TH varnish, differential scanning calorimetry (DSC) was used. Curing process was monitored with DSC850 by Mettler Toledo GmbH (Greifensee, Switzerland). Aluminium crucibles of 40  $\mu$ l, with a hole in the lid and around 8.5 mg of the material for each test, were used. Nitrogen flow was used as the purge gas, at 50 ml/min. In order to determine the total reaction enthalpy, non-isothermal scans were performed. The temperature was varied from 0 °C to 450 °C and the heating rates were 5, 10, 15 and 20 °C/min. Scans were analysed by Star software by Mettler Toledo

GmbH according to model free kinetic (MFK).

Once resins were cured (following the process stated in 2.1), the glass transition temperature ( $T_g$ ) was measured, also using DSC. In this case, a scan from 0 to 450 °C at 20 °C/min was carried out, and the  $T_g$  value was measured in the midpoint. DSC was carried out at 20 °C/min as it allows observation of small changes that would not be easy to find at lower heating rates, according to provider recommendations.

The decomposition kinetics of both cured epoxies (EP and TH) was evaluated with a Simultaneous Thermal Analyser (STA6000) from PerkinElmer (Massachusetts, United States) at four heating rates (10, 15, 17 and 20 °C/min) from 25 °C to 550 °C, in an air and nitrogen flow of 20 ml/min. Increasing testing temperature would not affect the decomposition temperature or the derivative of the thermogravimetric curves, which are the ones used to evaluate decomposition phenomena. The samples weighed from 16 to 18 mg and alumina crucibles of 60 µl were used without a lid. The MFK model can also be applied to calculate the decomposition energy ( $E_d$ ) of EP epoxy resin and TH epoxy varnish. The  $E_d$  at 5% decomposition was used to estimate the lifetime of epoxies by the Toop equation (Eq. (2)) [23] as a function of the operation service temperature.

$$\ln t_f = \frac{E_d}{RT_f} + \ln \left( \frac{E_d}{\beta R} P(X_f) \right) \quad (2)$$

where  $\beta$  is the heating rate,  $R$  is the gas constant,  $E_d$  is the decomposition energy calculated for a particular degradation degree (obtained from MFK),  $T_f$  is the chosen temperature to estimate lifetime,  $t_f$  is the estimated time until material failure and  $P(X_f)$  is a function which is controlled by  $E_d/RT_c$  values,  $T_c$  being the temperature at the decomposition degree which is considered for material failure, according to Toop tabulation [23].

### 2.3. Thermal conductivity

The thermal conductivity was determined by DSC, with a cycle from 20 to 38 °C at 0.5 °C/min, following the procedure established by Hakvoort and van Reijen [24], which is based on the stationary regime. This procedure involves putting a pure metal (e.g. indium or gallium) in an aluminium crucible on the material (EP, TH and EPTH) to be measured (without crucible), and both placed directly on the DSC sensor. A scheme of this technique is shown in Fig. 1. This method allows the obtainment of measurements with an uncertainty of about 5%.

Prisms with a squared basis of 3 mm side and an approximate height of 2 mm were prepared with EPTH. All measurements were repeated with different samples three times. The conductivity was measured according to Eq. (3), taking into account that the slope of the melting peak,  $S$ , is provided by Eq. 4

$$\lambda = \frac{\varphi}{\Delta T} \frac{h}{A} \quad (3)$$

$$\frac{\varphi}{\Delta T} = S \quad (4)$$

where:  $\varphi$  is the heat flow,  $A$  the base area of the prism,  $h$  is the height of the prism,  $\Delta T$  the temperature gradient, and  $S$  is the slope of the linear

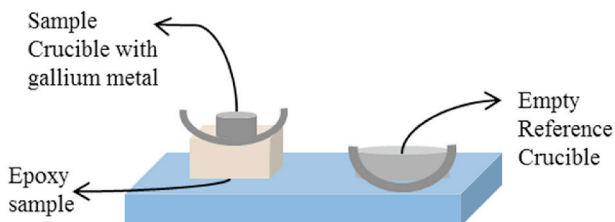


Fig. 1. Diagram of the thermal conductivity measurement by DSC.

part of the melting peak of the gallium metal.

### 2.4. Infrared spectroscopy

Fourier transform infrared (FTIR) spectra of materials were measured with a Bruker Vector 22 (Massachusetts, United States), equipped with attenuated total reflectance mode. The FTIR spectra of the uncured and cured samples were measured in the spectra range from 600 to 4000  $\text{cm}^{-1}$  and resolution 4  $\text{cm}^{-1}$ .

### 2.5. Durability

To evaluate the effect of moisture and temperature on the studied materials, the test specimens were exposed to two different aging conditions: 25 °C and 60 °C, always keeping 95% RH. 60 °C was chosen because class F and H are normally used when the ambient temperature is approximately 60 °C during operation [11]. Samples of EP and EPTH were exposed to the aging conditions for 35 days (840 h). Samples were weighed at different times (2, 24, 48, 72, 96, 168, 196, 384, 840 h) in order to evaluate water absorption by the relative uptake of weight,  $M_t$ , according to Eq. (5).

$$M_t = \frac{W_t - W_0}{W_0} \times 100 \quad (5)$$

where  $W_0$  is the weight of the dry specimen and  $W_t$  is the weight of the wet specimen at each aging time.

Although the sorption process of liquids and vapours in glassy polymers follows complex water diffusion mechanisms, this process has been frequently well approximated by Fickian diffusion laws for epoxy resins. This approximation is based on a semi-empirical equation (Eq. (6)) expressing the initial shape of sorption curves [25]. For a flat sheet of thickness  $h$  with uniform initial distribution and equal initial surface concentration, Fick's laws follow Eq. (6) [26]:

$$\frac{M_t}{M_m} = 1 - \frac{8}{\pi^2} \sum_{n=0}^{\infty} \frac{1}{(2n+1)^2} \exp \left[ \frac{-(2n+1)^2 \pi^2 D t}{h^2} \right] \quad (6)$$

where  $M_t$  is the moisture uptake at time  $t$ ,  $M_m$  is its maximum moisture uptake at equilibrium state,  $D$  is the diffusivity and  $h$  is the thickness of the specimen.

Depending on  $M_t/M_m$  values, some approximations are reported [27]. When  $M_t/M_m$  is lower than 0.6, the initial part of the curve can be correlated to Eq. (7):

$$\frac{M_t}{M_m} = \frac{4}{h} \sqrt{\frac{Dt}{\pi}} \quad (7)$$

For  $M_t/M_m$  values higher than 0.6, a good approximation is shown with following Eq. (8):

$$\frac{M_t}{M_m} = 1 - \exp \left[ -7.3 \left( \frac{Dt}{h^2} \right)^{0.75} \right] \quad (8)$$

Diffusion coefficient,  $D$ , is the most important parameter and should be calculated with Eq. (7) or 8 for each case, depending on  $M_t/M_m$  values.

In general, epoxies lose part of their properties when they absorb water. The initial properties can be partially recovered by means of a drying stage at RT and controlled humidity [27]. In this research, DSC measurements were performed directly after the end of the aging conditions (35 days exposure) on materials without drying, to measure their  $T_g$ .

### 3. Results and discussion

#### 3.1. Glass transition temperatures

Curing processes were performed according to the industrial criteria; in this case EP and TH were separately cured for 10 h at 140 °C. Besides, EP was cured a second time at 140 °C for 10 h, since industrially it is cured again when it is varnished with TH.

Fig. 2A shows the DSC curves of EP after one and two curing processes. After the first curing process at 140 °C for 10 h, three  $T_g$ s are found (at 77, 112 and 250 °C). At 306 °C, a small exothermal reaction peak ( $\Delta H = 5$  J/g), due to the curing reaction, appears. It is followed by another exothermal reaction peak ( $\Delta H = 78$  J/g), where curing is overlapped with a decomposition peak at 430 °C, so they cannot be separated. This means that the EP does not fully cure with the selected curing process. After the second curing process (140 °C -10 h), the DSC curve presents four  $T_g$ s (at 99, 134, 237 and 294 °C). At 332 °C, a small exothermic reaction peak is still observed, with an enthalpy of only 2 J/g. A decomposition peak at 429 °C ( $\Delta H = 74$  J/g) is also observed (as in point 3.3 is shown, the peak can be attributed to decomposition because it coincides with the beginning of the decomposition in the STA, approximately).

Fig. 2B corresponds to the DSC curve for TH after a curing process (140 °C - 10 h). As for EP, it also shows a  $T_g$  at 73 °C overlapped to a small endothermal relaxation effect or evaporation peak, which is followed by a small exothermal peak at 119 °C (0.63 J/g) and a broad exothermal curing peak at 252 °C ( $\Delta H = 44.5$  J/g). A decomposition peak is also found (44.80 J/g) at 391 °C. A second heating was not carried out, because TH decomposed in the first heating. It is curious that both enthalpies are equal; this seems that there is a part of TH which has not decomposed. This can be due to relation of  $T_g$  peak to evaporation that agrees with the strong odour released.

To be able to study the  $T_g$  of TH, two scans at lower temperature, from 0 to 350 were carried out consecutively. In the first scan after 10 h at 140 °C,  $T_g$  and curing peak were observed at 73 °C and 252 °C respectively (as Fig. 2B). However, in the second scan  $T_g$  at 115 °C was

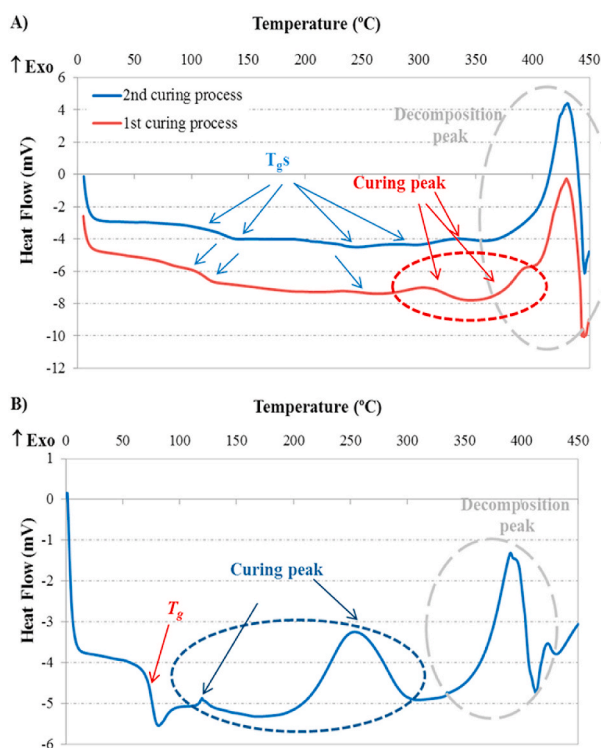


Fig. 2. DSC to measure glass transition temperatures for A) EP and B) TH.

only shown and TH is totally cured.

#### 3.2. Curing reaction: kinetics

Fig. 3A shows the DSC for a heating of 20 °C/min of the uncured EP sample. It was heated up to 450 °C. At low temperature, it shows two overlapped peaks at 152 and 187 °C which correspond to curing peaks that will be studied in Fig. 4.

A high exothermal peak is found at 405 °C (Fig. 3A), whose enthalpy is 374 J/g. Decomposition peak in  $T_g$  DSCs (Fig. 2A) has  $\Delta H = 74$  J/g (in the second curing process); this difference of around 300 J/g could mean that, inside the decomposition peak, there is a part related to curing. Considering the 300 J/g difference, the decomposition peak observed at high temperature in Fig. 3A is only equivalent to around 38%. According to deconvolution carried out in Fig. 3A on the final peak (Fig. 3B), it can be split into two. On the one hand, the curing peak at 385 °C is equivalent at 61.5% and on the other hand the peak of 38.5% at 403 °C corresponds to the decomposition peak.

The activation energy by the MFK method can only be calculated at the two initial peaks, since the software cannot work on the peak comprising overlapping both curing and decomposition processes; consequently, only the non-isothermal scans up to 350 °C are shown in Fig. 4.

The curves (Fig. 4) are shifted to lower temperatures when the test rate increases. These shifts are always found for flow heat vs time curves when heating rates change. The two peak temperatures are also shifted as shown in Table 1. Besides, the enthalpy of the whole curing process ( $\Delta H_C$ ) should be the same for all rates, being obtained  $185 \pm 1$  J/g for EP (Table 1). The homogeneity in the  $\Delta H_C$  values and the shifting of the curves with the rate is a first step to consider the curves as valid. The presence of two peaks in the DSC for the epoxy can be understood as two different components which can be present in this single-component

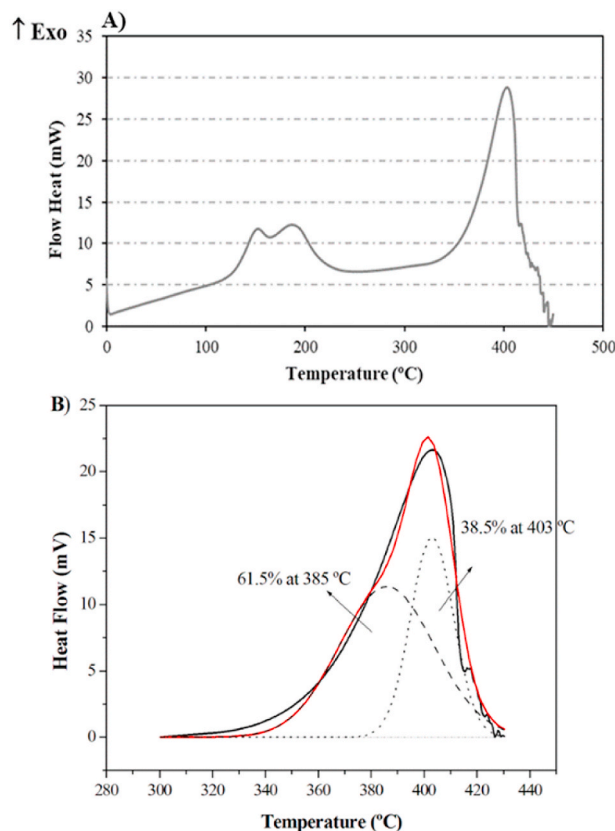


Fig. 3. A) Non-isothermal curves by DSC at 20 °C/min for EP. B) Deconvolution of decomposition peak at 20 °C/min (peak at higher temperature in Fig. 3A).

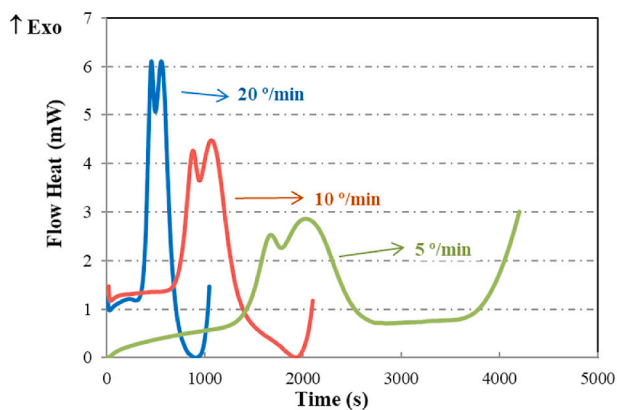


Fig. 4. Non-isothermal curves by DSC at different rates for EP.

Table 1  
Curing peak temperatures and  $\Delta H_c$  for EP.

Curing rate (°/min)	Curing peaks		$\Delta H_c$ (J/g)
	Temperature (°C)		
	1st peak	2nd peak	
20	152	187	184.4
10	145	178	185.6
5	138	174	184.8

resin, while being usual with only one peak during the non-isothermal curing of a bi-component epoxy [28].

The last concept to take into account for validating the curing curves is shown by the conversion curves. These curves are derived from the curve of curing vs. temperature. Curing curves are shown in Fig. 5A,

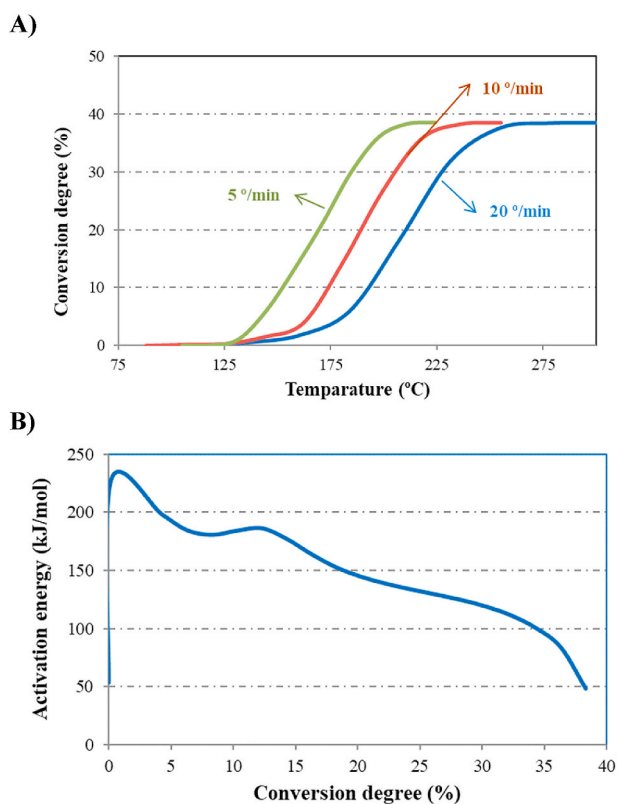


Fig. 5. A) Conversion degree curves at different rates for EP and B) Activation energy versus conversion degree for EP.

where the influence of test rate is once again evident in shifting the curves to higher temperatures. Since they do not cross over, the MFK model can be applied.

From conversion degree curves, the activation energy is calculated as a function of the conversion degree. Fig. 5B shows the activation energy versus conversion degree of EP. At the beginning, the reaction needs a high  $E_a$  (228 kJ/mol) and it decreases throughout the process, once the reaction has already started. An increment of activation energy up to 173 kJ/mol at approximately 13% conversion degree is observed, that corresponds to the second peak of the curves of curing (Fig. 3A). Afterwards,  $E_a$  continues decreasing until a 38.5% conversion degree occurs (50 kJ/mol). This first part of the reaction is in accordance with the  $n$  order mechanism (slower) up to about 30% of the reaction [29,30], when the process needs more  $E_a$ . The typical autocatalytic mechanism of bi-component epoxies, taking place when the oxirane ring opens (usually from 30% to 80% conversion degree), cannot be observed in Fig. 5B since it is a mono-component epoxy, in this case an autocatalytic mechanism appears from 13 to 38%.

Usually, at the end of this type of reactions, most oxirane rings have reacted involving an increase of the  $E_a$  to the finish of the curing process, and the mechanism would follow the  $n$  order again. The EP will need a contribution of high energy to reach the end of the reaction, which agrees with a  $T_g$  at a higher temperature, but it cannot be calculated by the MFK model and another method is needed. The extra activation energy that the EP resin needs to finish its curing entirely is 124 kJ/mol and this can be calculated by the Kissinger method (Eq. (9)), where  $\beta$  is the heating rate,  $T$  is the curing peak temperature (K) (see Fig. 3B), and  $R$  the gas constant (8.314 J/mol·K).

$$\ln\left(\frac{\beta}{T^2}\right) = -E_a/RT + C \tag{9}$$

In this contribution of energy, time also has an effect, thus, for this reason, two curing processes at 140 °C for 10 h each are usually employed in industrial applications. This avoids having to raise temperature substantially and therefore the decomposition temperature is not reached.

When the  $E_a$  is already calculated, the software allows the simulation of isothermal curing curves (Table 2). In this case, the heating processes have been simulated for high curing temperature. Industrially, EP is cured at 140 °C for 10 h and regarding Table 2, at this temperature, EP is able to cure in an hour, which would imply an important saving time compared to the industrial process. However, as already commented, the curing process of EP is not completely finished in 10 h with 61.5% of resin remaining uncured (Fig. 3B), so the simulation was done until 38.5% conversion.

Curing curves of TH are totally different; when tests are performed at 20 °C/min, the DSC curve (Fig. 6) shows a  $T_g$  at 114 °C overlapped to an endothermal relaxation effect or evaporation peak and followed by an evaporation peak at 155 °C, ( $\Delta H = 6$  J/g). Then a broad exothermal curing peak is observed at 180 °C ( $\Delta H_c = 65$  J/g), followed by a

Table 2  
Simulation of isothermal curing for EP until 38.5%.

Applied Kinetics: Conversion					
Conversion degree (%)	Temperature (°C)				
	120	130	140	150	160
	Time (min)				
5	14.51	3.38	0.85	0.39	0.42
10	49.76	12.37	3.29	0.93	0.46
15	97.87	41.88	12.05	3.68	1.19
20	97.92	68.46	23.92	8.78	3.38
25	97.97	69.95	40.94	16.48	6.92
30	98.02	70.00	50.79	28.15	12.80
35	98.07	70.05	50.85	37.45	21.58
38	98.10	70.08	50.89	37.51	26.62

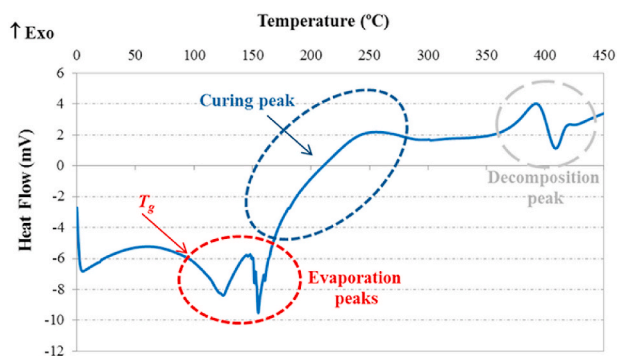


Fig. 6. Heating curve at 20°/min for uncured TH.

decomposition peak at 393 °C ( $\Delta H = 22 \text{ J/g}$ ). Testing at 15°/min shows a wider  $T_g$  (from 83 to 109 °C), at 93 °C, overlapped with an endothermal relaxation or evaporation peak.  $T_g$  is followed by a small endothermal evaporation peak at 156 °C ( $\Delta H = 3 \text{ J/g}$ ). Afterwards, a broad exothermal peak at 233 °C ( $\Delta H_c = 67 \text{ J/g}$ ) and a decomposition peak at 387 °C ( $\Delta H = 23 \text{ J/g}$ ) are found. Similar results are seen with heating performed at 10 °C/min.

The  $\Delta H_c$  for both rates are similar, however the  $T_g$  is different when heating rates change. A difference in temperature of about 7 °C can be assumed because it could be due to the different test rate, but in this case the difference is higher, around 15 °C. This can be associated with the evaporation of the solvent. At 15 °C/min, the solvent is released more slowly and the evaporation peak is not clearly defined since the  $T_g$  zone is wider. Furthermore, when the  $T_g$  of the TH was studied in the first heating process (Fig. 2B), it was 73 °C. Fig. 6 confirms that the final peak shown in Fig. 2B (with a heat of 45 J/g) corresponds to the decomposition peak. In any case, it could be observed that initially the TH plus solvent has a higher  $T_g$  than when there is no solvent.

If the difference between curing and decomposition enthalpies (Fig. 6) is about 44 J/g, it corresponds with the curing peak enthalpy after 10 h at 140 °C shown in Fig. 2 B, in which case the decomposition peak enthalpy was equal to the curing peak. The total enthalpy curing process is 88 J/g, which means that 25% is pre-polymerized and after 10 h at 140 °C the extent of cure is around 48%, with solvent evaporation depending on heating rate. In this way, the conversion degree curves intersect and MFK cannot be applied.

### 3.3. Decomposition process: kinetics

The STA test on the EP resin (Fig. 7) shows a curve where there is a slight decrease from 365 to 424 °C that corresponds with the beginning of the decomposition process [31,32]. This temperature range

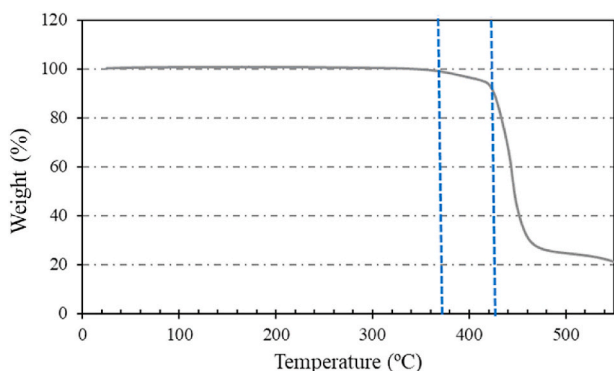


Fig. 7. STA decomposition curve at 20°/min for EP.

corresponds to the DSC peaks attributed to decomposition, 403 °C in Figs. 3B and 429 °C in Fig. 2A, and it represents around 5% of decomposition. All curves studied show the same aspect, although they are shifted according to heating rate.

STA curves were derived to apply the MFK model, then they were treated in the same way as DSC curves already studied (in section 3.2). Thus, conversion degree curves and  $E_d$  curve versus conversion degree were obtained.

The  $E_d$  curve allows simulation of the isothermal curves at different temperatures and times. Lifetime estimation was calculated at 5% conversion degree according to Eq. (1) for EP and TH separately (Fig. 8), since 5% is the decomposition percentage that was determined as the beginning of decomposition (zone between the discontinued straight lines in Fig. 7). The EPTH is not able to be analysed because decomposition of all products is overlapped.

Fig. 8 shows that EP has a lifetime estimation less than TH at all temperatures, but at 175 °C they are closer. At this temperature the TH varnish has a lifetime estimation around 143 years and for the EP is 26 years. Regarding the EPTH system and its working temperature, and according to other researchers who have estimated the lifetime of epoxy insulation around 37 years at 250 V [12], the obtained lifetime is approximately the life in service of a transformer. Therefore, it seems like this lifetime estimation is correct.

### 3.4. Thermal conductivity

Thermal conductivity was measured for EP, TH and the whole system, EPTH, after their corresponding curing processes. Fig. 9 shows the melting peak of gallium when the epoxy prisms are blocking the thermocouple signal.

The smallest melting peak for gallium corresponds to TH. EP provides the biggest peak and an intermediate peak is obtained for the EPTH. However, the slope of these peaks is what provides the thermal conductivity through Eqs. (3) and (4). Once these equations are applied, Fig. 10 shows the thermal conductivities. The TH varnish decreases the thermal conductivity of the EP when they are working together (EPTH), although this decrease is small, since the varnish layer is thin compared to the EP prism. The EP value could be compared to other epoxy resins such as Epofer, which shows a thermal conductivity of  $0.16 \text{ Wm}^{-1}\text{K}^{-1}$ , when measured in the same way [33].

### 3.5. Infrared spectroscopy

Fig. 11 shows the infrared spectra for both uncured and cured epoxies. The most significant bands of an epoxy are those corresponding to the oxirane group. These bands are ring vibration from 775 to 950  $\text{cm}^{-1}$ , C-O stretching vibration from 1230 to 1280  $\text{cm}^{-1}$ , C-H stretching from 2990 to 3000  $\text{cm}^{-1}$  and C-H asymmetric stretching vibration from 3030 to 3075  $\text{cm}^{-1}$  [34]. Besides, it contains other vibrations depending on its organic chain.

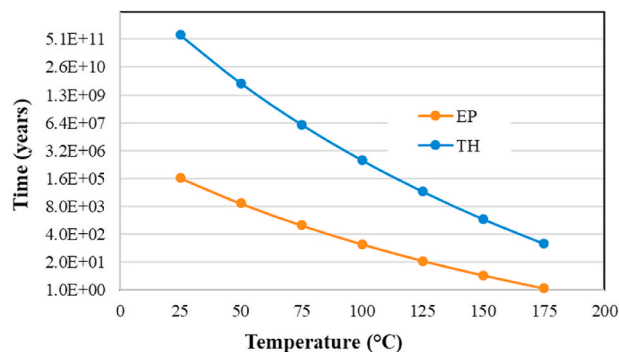


Fig. 8. Life estimation for EP and TH.

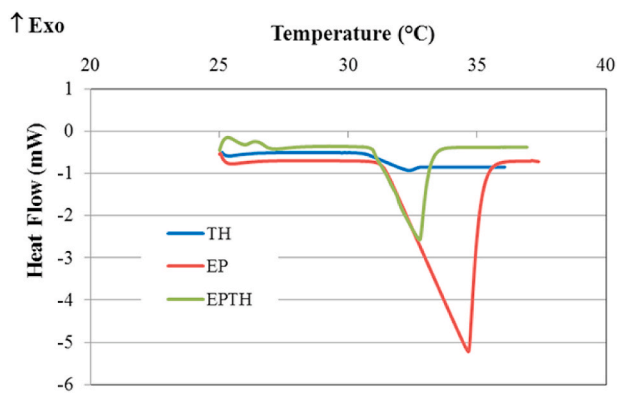


Fig. 9. Heating curves to measure thermal conductivity.

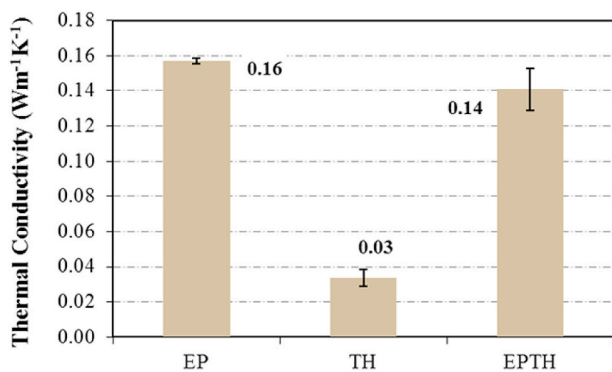


Fig. 10. Thermal conductivity for EP, TH and EPTH.

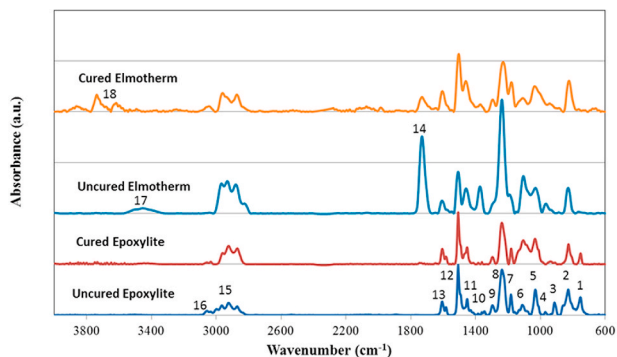


Fig. 11. Normalized absorbance as a function of wavenumber (cm-1) for EP and TH uncured and cured.

The band at 1035 cm<sup>-1</sup>, corresponding to the aromatic ring of the bisphenol, is not affected by the curing reaction and was used as a reference, with all spectra normalized in relation to this band. The band at 915 cm<sup>-1</sup> is characteristic of the oxirane ring which changes during curing process, and which disappears after curing.

The assignment of the bands in the spectra is displayed in Table 3. In general EP and TH show the typical bands found in other epoxies. The main difference between EP and TH is the band found at 914 cm<sup>-1</sup> (band number 3). This band does not appear in uncured TH, what means varnish is already cured before the curing process. This brings up again Figs. 2B and 6, considering that curing peaks are appearing. It seems that oxirane rings are opened, what agrees with a bigger peak (number 8 in Fig. 11 and Table 3) at 1236 cm<sup>-1</sup> (C-O str) and more OH groups (number 17 in Fig. 11 and Table 3), and the solvent is blocking the curing reaction. This can be produced, since although the oxirane rings are opened,

Table 3  
Assignations of bands corresponding to the shown spectra on Fig. 11 [34].

	Wavenumber (cm <sup>-1</sup> )	Type of Vibration	EP		TH	
			Uncured	Cured	Uncured	Cured
1	756	C-H def	*	*		
2	830		*	*	*	*
3	914	C-O-C ring	*			
4	972	C=C-H def	*			
5	1032	C-O-C str AR	*	*	*	*
6	1115	C-O-C str	*	*	*	*
7	1185	H-C-H Bd	*	*	*	*
8	1236	C-O str	*	*	*	*
9	1298	H-C-H Bd	*	*	*	*
10	1375	H-C-H Bd	*	*	*	*
11	1450	H-C-H Bd	*	*	*	*
12	1510	C-C AR	*	*	*	*
13	1602	C=C str	*	*	*	*
14	1730	C=O str			*	*
15	2800-3000	C-H str	*	*	*	*
16	3060	C-H asym str	*	*		*
17	3200-4000	C=N/C=N-			*	*
18		OH/OH/N-H str				*

Ar: Aromatic; def: deformation; str: stretching; Bd: bending.

as solvent can block the nucleophilic amino groups, which would prevent the cross-linking and growth of the chains.

Regarding bands number 17 and 18, it can be affirmed that TH is dissolved in some ether-type dioxane, since these bands can be assigned to free O-H stretching vibration in dilute solution. The band number 11 is also associated with an O-H deformation vibration. All of these bands are characteristics of ether functional groups. Besides, ethers show a strong absorption band in the range 1270-1060 cm<sup>-1</sup> (band number 8), that can be found in the uncured TH spectrum. Another important difference is the carbonyl group (band 14), assigned for TH but not in EP, although this band is usually found in epoxy resins.

### 3.6. Durability

The durability of the EPTH system was studied at 25 °C - 95% RH and 60 °C - 95% RH. The samples were introduced into the climatic chamber for 840 h. Fig. 12 shows the weight gain versus time for both conditions.

As expected, increasing temperature has a meaningful effect on water absorption. The samples exposed to 60 °C - 95% RH presents greater water absorption than at 25 °C - 95% RH. Both conditions show a fast water uptake at the beginning of the aging time, and then the water uptake is slower. It can also be stated that samples subjected to 60 °C reached the maximum water uptake around 168 h, since from here until the end of the aging time the last four weight measurements were practically the same. Samples at 25 °C did not reach this saturation value

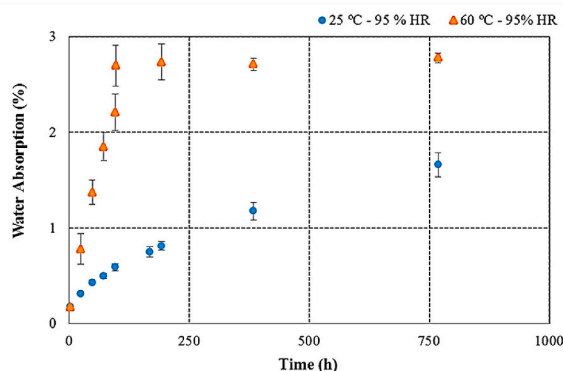


Fig. 12. Water absorption vs time for EPTH at different conditions.

even at the end of the 35 days. This value is 2.785% and was established as  $M_m$  for the calculation of diffusivity. Table 4 shows the diffusion coefficient for EPTH under both conditions. The diffusion coefficient for EPTH is greater under the more aggressive condition because the higher temperature supports water absorption and enhances the diffusion process.

DSC tests of EPTH were performed after 35 days of aging.  $T_g$  values obtained were compared with those obtained for EP and TH as shown in Table 5.

According to Fig. 2A, EP presents four  $T_g$ s at 99, 134, 237 and 294 °C, that should be found in the unaged sample of the EPTH system. When EP is varnished with TH, it is difficult to find four  $T_g$ s because they are overlapped. The EPTH sample which did not undergo aging shows a  $T_g$  at 74 °C, which corresponds to TH (Fig. 2B), followed by three  $T_g$ s at 107, 130 and 219 °C slightly displaced with respect to the  $T_g$ s of EP in the 1st curing process (Fig. 2A). The highest  $T_g$  (294 °C) cannot be found since it probably coincides with a curing peak at 301 °C ( $\Delta H_c = 7$  J/g) of the TH. Regarding DSC results, it is observed that when EPTH is subjected to 25 °C-95% RH aging conditions, four  $T_g$ s are observed at 62 (TH), 107, 132 and 218 °C. These  $T_g$ s are like the unaged EPTH. However, when it is subjected to 60 °C and 95% RH, all the  $T_g$ s decrease considerably with the highest  $T_g$  disappearing. The presence of absorbed water is slightly observed in the first  $T_g$  at 25 °C and 95% RH as a small endothermal relaxation. Comparing now the diffusion coefficients obtained for the EPTH, it can be seen, on one side, that diffusivity is greatly favoured by the high temperature, and on the other side, the protection effect of TH against humidity.

At 25 °C it is observed that diffusivity is lower because of the protective effect of the TH. However, at 60 °C this TH protection is not observed. This may be due to the fact that TH has started to degrade at 60 °C (hence its  $T_g$  is much lower) and therefore does not offer the protection it should. This means there is a plasticization effect due to free water occupying free space within the polymer, which would agree with the small endothermal relaxation which overlapped with  $T_g$  at 25 °C and 95% RH; but it would disagree at 60 °C and 95% RH, where it is possible that another mechanism, for example involving bound water, forming single or multiple hydrogen bonds with the polymer chain, resulting in this case in swelling, plasticization and decreasing both strength and glass transition temperature [35]. Even so, when this system is compared with other epoxy resins, the water absorption is lower. For example Barbosa et al. [36] found that samples immersed in water at 50 °C had a water saturation value of 5.8%. The studied materials have shown an excellent moisture performance, specially taking into account the most aggressive conditions of ambient humidity than immersion conditions, as diffusion is faster in the former due to the smaller size of water molecule.

#### 4. Conclusions

Thermal kinetic and water diffusion studies of two epoxy resins used as insulation in electrical transformers has been carried out. After an analysis of the curing processes it can be affirmed that the curing process suggested for the industry is necessary and EP needs all time necessary for a progressive curing.

Thermal analysis of the curing process of TH has revealed that TH is a prepolymer in the presence of solvents. This was supported by FTIR-ATR where the process has been stopped by solvent with the oxirane rings already opened.

The life in service of both resins was calculated obtaining higher values for the TH than for the EP, so TH acts as a protector of EP. If service temperature is above 170 °C the estimated lifetimes of both EP and TH are very similar.

This protective effect is also seen in the water absorption tests, obtaining lower diffusion coefficients when the EP is covered by the TH. However, the degradation of TH starts at 60 °C and the protective effect against humidity disappears.

**Table 4**

$T_g$  Diffusion coefficients for EPTH.

	Aged	
	25 °C - 95 %RH	60 °C - 95 %RH
Diffusion coefficient (cm <sup>2</sup> /s)	2.28E-09	2.92E-08

**Table 5**

Aging effect on  $T_g$ .

$T_g$ (°C)	EP	TH	Unaged	EPTH	
				25 °C - 95 %RH	60 °C - 95 %RH
		73	74	62	46
	99		107	107	97
	134		130	132	134
	237		219	218	
	294				

The TH varnish also acts as an attenuator of the thermal conductivity, slightly reducing the conductivity of the EP when it is varnished with the TH.

Therefore, to sum up, the EPTH protective system is entirely suitable for the isolation of electrical transformers taking into account that class H is used when the ambient temperature is of the order of 60 °C or so during operation.

Degradation observed on TH agrees with the fact that, every so often, electrical transformers are impregnated with TH varnish several times.

#### Funding

This research was funded by European Union's Horizon 2020 research and innovation programme under grant agreement No 766437 (ESSIAL project).

#### Acknowledgments

The authors acknowledge the technical support given by the Chemistry Laboratory of Mechanical Engineering Department of Comillas Pontifical University - ICAI of Madrid.

#### References

- [1] Fofana I. 50 years in the development of insulating liquids. *IEEE Electr Insul Mag* 2013;29(5):13–25. <https://doi.org/10.1109/MEI.2013.6585853>.
- [2] Ford JG. Paper insulation for transformers. 1965. Patent US3246271A USA.
- [3] EN 60529. Degrees of protection provided by enclosures (IP Code). 1991.
- [4] Dakin TW. Application of epoxy resins in electrical apparatus. *IEEE Tms Dielect. Electr Insul* 1974;9(4):121–8. <https://doi.org/10.1109/TEI.1974.299321>.
- [5] Jyothi NS, Ramu TS, Mandlik M. Temperature distribution in resin impregnated paper insulation for transformer bushings. *IEEE Tm Dielect Electr Insul* 2010;17(3):931–8. <https://doi.org/10.1109/TDEI.2010.5492269>.
- [6] Van Der Linde D, Boon CAM, Klaassens JB. Design of a high-frequency planar power transformer in multilayer technology. *IEEE Tms Ind Electron* 1991;38(2):135–41. <https://doi.org/10.1109/41.88907>.
- [7] Borsi H. The relation between thermal and electrical stress and the PD behavior of epoxy-resin transformers. *IEEE Tms Electr Insul* 1993;28(6):1007–15. <https://doi.org/10.1109/14.249374>.
- [8] Hikita M, Kozako M, Takada H, Hirose T, Higashiyama M, Nakamura S, Umemura T. Partial discharge phenomena in artificial cavity in epoxy cast resin insulation system. In: *IEEE Int Symp Electr Insul*. San Diego, CA; 2010. p. 5. <https://doi.org/10.1109/ELINSL.2010.5549549>.
- [9] Illias HA, Chen G, Lewin PL. The influence of spherical cavity surface charge distribution on the sequence of partial discharge events. *J Phys D Appl Phys* 2011;44(24). <https://doi.org/10.1088/0022-3727/44/24/245202>.
- [10] IEC 60034-1. Rotating electrical machines – Part 1: rating and performance. 2010.
- [11] Raman B. Winding insulation and its maintenance. *Newnes Power Engineering Series*. In: Agrawal KC, editor. *Industrial power Engineering and applications Handbook*. Massachusetts, USA: Butterworth-Heinemann publications; 2001 [chapter 9].
- [12] Zhuang Q, Morshuis PHF, Chen X, Meijer S, Smit JJ, Xu Z. Life prediction for epoxy resin insulated transformer windings through accelerated aging tests. In: *Proc the*

- IEEE Int Conference solid Dielectr. Postdam, Germany; 2010. p. 1–4. <https://doi.org/10.1109/ICSD.2010.5567921>.
- [13] Henk PO, Kortsen TW, Kwarts T. Increasing the electrical discharge endurance of acid anhydride cured DGEBA epoxy resin by dispersion of nanoparticle silica. *High Perform Polym* 1999;11:281–96. <https://doi.org/10.1088/0954-0083/11/3/304>.
- [14] Raquez JM, Deléglise M, Lacrampe MF, Krawczak P. Thermosetting (bio) materials derived from renewable resources: a critical review. *Prog Polym Sci* 2010;35:487–509. <https://doi.org/10.1016/j.progpolymsci.2010.01.001>.
- [15] Paz-Abuín S, López-Quintela A, Pazos-Pellín M, Paz-Pazos M. Influence of the reactivity of amine hydrogens and the evaporation of monomers on the cure kinetics of epoxy-amine: kinetic questions. *Polymer* 1997;38:3795–804. [https://doi.org/10.1016/S0032-3861\(96\)00957-3](https://doi.org/10.1016/S0032-3861(96)00957-3).
- [16] Bandyopadhyay A, Odegard G. Molecular modeling of crosslink distribution in epoxy polymers. *Model Simulat Mater Sci Eng* 2012;20(4). <https://doi.org/10.1088/0965-0393/20/4/045018>.
- [17] Ratna D. *Handbook of Thermoset resins*. United Kingdom: iSmithers – A Smithers Group Company; 2009.
- [18] Kamal MR, Sourour S. Kinetics and thermal characterization of thermoset cure. *Polym Eng Sci* 1973;13:59–64. <https://doi.org/10.1002/pen.760130110>.
- [19] Kissinger HE. Reaction kinetics in differential thermal analysis. *Anal Chem* 1957;29:1702–6. <https://doi.org/10.1021/ac60131a045>.
- [20] Vyazovkin S. Advanced isoconversional method. *J Therm Anal Calorim* 1997;49:1493–9. <https://doi.org/10.1007/BF01983708>.
- [21] Abenojar J, Martínez MA, Velasco F, Rodríguez-Pérez MA. Atmospheric plasma torch treatment of polyethylene/boron composites: effect on thermal stability. *Surf Coating Technol* 2014;239:70–7. <https://doi.org/10.1016/j.surfcoat.2013.11.020>.
- [22] Xu J, Bhattacharya S, Pramanik P, Pramanik P, Wong C. High dielectric constant polymer-ceramic (epoxy varnish-barium titanate) nanocomposites at moderate filler loadings for embedded capacitors. *J Elec.Mater* 2006;35. <https://doi.org/10.1007/s11664-006-0307-6>. 2009–15.
- [23] Toop DJ. Theory of life testing and use of thermogravimetric analysis to predict the thermal life of wire enamels. *IEEE Tms Electr Insul* 1971;6:2–14. <https://doi.org/10.1109/TEI.1971.299128>.
- [24] Hakvoort G, Van Reijen LL. Measurement of the thermal conductivity of solid substances by DSC. *Thermochim Acta* 1985;93:317–20. [https://doi.org/10.1016/0040-6031\(85\)85081-4](https://doi.org/10.1016/0040-6031(85)85081-4).
- [25] Liu M, Wu P, Ding Y, Li S. Study on diffusion behavior of water in epoxy resins cured by active ester. *Phys Chem Chem Phys* 2003;5:1848–52. <https://doi.org/10.1039/b208782k>.
- [26] Comyn J. *Polymer Permeability*. London, UK: Elsevier Applied Science; 1985.
- [27] Frigione M, Aiello MA, Naddeo C. Water effects on the bond strength of concrete/concrete adhesive joints. *Construct Build Mater* 2006;20:957–70. <https://doi.org/10.1016/j.conbuildmat.2005.06.015>.
- [28] Roşu D, Caşcaval CN, Mustată F, Ciobanu C. Cure kinetics of epoxy resins studied by non-isothermal DSC data. *Thermochim Acta* 2002;383:119–27. [https://doi.org/10.1016/S0040-6031\(01\)00672-4](https://doi.org/10.1016/S0040-6031(01)00672-4).
- [29] Abenojar J, Encinas N, del Real JC, Martínez MA. Polymerization kinetics of boron carbide/epoxy composites. *Thermochim Acta* 2014;575:144–50. <https://doi.org/10.1016/j.tca.2013.10.030>.
- [30] Abenojar J, Martínez MA, Pantoja M, Velasco F, del Real JC. Epoxy composite reinforced with nano and micro SiC particles: curing kinetics and mechanical properties. *J Adhes* 2012;88:418–34. <https://doi.org/10.1080/00218464.2012.660396>.
- [31] Song IK, Lee BS, Jung JW, Kim SJ. Thermal analysis of varnish treated insulating papers for transformers. In: *Proc: Electr Insul Conf Electr Manuf Coil winding Technol Conf*. (Cat. No.03CH37480), Indianapolis, USA; 2003. p. 583–6. <https://doi.org/10.1109/EICEMC.2003.1247952>.
- [32] Interpreting unexpected events and transitions in DSC results, TA instrument TA039. Available online: [www.tainstruments.com/pdf/literature/TA039](http://www.tainstruments.com/pdf/literature/TA039). [Accessed 16 September 2019].
- [33] Abenojar J, Pantoja M, Martínez MA, del Real JC. Aging by moisture and/or temperature of epoxy/SiC composites: thermal and mechanical properties. *J Compos Mater* 2015;49:2963–75. <https://doi.org/10.1177/0021998314558496>.
- [34] Socrates G. *Infrared and Raman characteristic group frequencies*. West Sussex, England: John Wiley & Sons, LTD.; 2001.
- [35] Viana G, Costa M, Banea MD, da Silva LFM. A review on the temperature and moisture degradation of adhesive joints. *Proc Ind Mech Eng Part L: J Mater: Des Appl*. 2016;231(5):488–501. <https://doi.org/10.1177/1464420716671503>.
- [36] Barbosa AQ, da Silva LFM, Öchsner A. Hygrothermal aging of an adhesive reinforced with microparticles of cork. *J Adhes Sci Technol* 2015;29:1714–32. <https://doi.org/10.1080/01694243.2015.1041358>.